

Studies of the pulse charge of lead-acid batteries for PV applications Part I. Factors influencing the mechanism of the pulse charge of the positive plate

A. Kirchev*, M. Perrin, E. Lemaire, F. Karoui, F. Mattera

*Commissariat de l'Energie Atomique, Institut National de l'Energie Solaire, INES-RDI, Parc Technologique de Savoie Technolac,
50 Avenue du Lac Léman, 73377 Le Bourget du Lac Cedex, France*

Received 30 July 2007; received in revised form 28 September 2007; accepted 27 October 2007

Available online 17 November 2007

Abstract

The mechanism of the positive plate charge in pulse regime was studied in model lead-acid cells with one positive and two negative plates (8 Ah each) and Ag/Ag₂SO₄ reference electrodes. The results showed that the evolution of the electrode potential is much slower on the positive plate than on the negative plate. Regardless of this fact, the calculated capacitive current of charge and self-discharge of the electrochemical double layer (EDL) during the “ON” and “OFF” half-periods of the pulse current square waves is comparable with the charge current amplitude. The result is due to the high values of the EDL on the surface of the lead dioxide active material. The influence of different factors like state of charge, state of health, pulse frequency, current amplitude and open circuit stay before the polarization was discussed. The previously determined optimal frequency of 1 Hz was associated with a maximum in the average double layer current on frequency dependence. The average double layer current is also maximal at SOC between 75 and 100%. The exchange of the constant current polarization with pulse polarization does not change substantially the mechanism and the overvoltage of the oxygen evolution reaction on the positive plate. The mechanism of the self-discharge of the EDL was also estimated analyzing long-time PPP transients (up to 2 h). It was found that when the PPP is lower than 1.2 V the preferred mechanism of EDL self-discharge is by coupling with the lead sulphate oxidation reaction. At higher values of PPP the EDL self-discharge happens via oxygen evolution. The high faradic efficiency of the pulse charge is due to the chemical oxidation of the Pb(II) ions by the O atoms and OH radicals formed at the oxygen evolution both during the “ON” and “OFF” periods.

© 2007 Elsevier B.V. All rights reserved.

Keywords: Lead acid; Pulse charge; Electrochemical double layer; Oxygen evolution

1. Introduction

One of the most severe problems of the lead-acid batteries operating in solar energy storage applications is the lack of charge due to the intermittent current from the photovoltaic (PV) module. The insufficient charge results often in hard sulphation of the positive plate [1], when the cells are flooded, and sulphation of both plates, when the cells are valve-regulated [2]. Recently a new charge strategy was proposed to overcome the

insufficient charge of the lead-acid batteries for PV-storage [3]. The strategy consists of two-step charge algorithm—the first step is galvanostatic until a certain cell voltage limit is reached and the second step is pulse-current (or interrupted-current) charge for a fixed amount of time. It was found that the application of the pulse-current step in this algorithm reduces substantially the quantity of the residual PbSO₄ at the end of the charge.

In the literature, the first studies concerning the pulse charge of lead-acid battery are directed towards its application for rapid charge of traction cells for electric vehicles [4–6]. The results show that the rate of the charge can be accelerated substantially down to 30–60 min for the full charge of an empty battery without substantial loss of energy. More recent studies show other advantages of the rapid pulse charge: it can be used to overcome negative phenomena limiting the exploitation period of

* Corresponding author at: CEA-INES, Laboratory of Solar Systems, 50 Avenue du Lac Léman, INES-RDI BP 332, 73377 Le Bourget du Lac, France. Tel.: +33 4 79 44 45 49; fax: +33 4 79 68 80 49.

E-mail address: angel.kirchev@cea.fr (A. Kirchev).

the battery such as premature capacity loss (PCL) effect [7], to increase the cycle life of the battery [8], to suppress the sulphation of the negative plates in VRLA cells and to avoid the thermal runaway phenomenon [2,9,10], and to restore the capacity of batteries after sulphation [11]. Using pulse charge, a decrease and time delay of the oxygen evolution during the charge of VRLA cells have been reported [12]. Despite of the numerous publications on the positive impact of pulse charging, theoretical studies of the processes taking place during the pulse charge are a rather new topic. In 1999 Guo et al. proposed a diffusion kinetics theory of the pulse charge of the positive plate of VRLA cells with and without voltage limitation [13]. In 2000 Kim and Hong [14] performed a simulation of rapid pulse charge of lead-acid cell. They demonstrated that the influence on the depolarization of both plates of the rest and the discharge periods during the pulse charge is a result of the reduced concentration gradients of the H^+ , HSO_4^- and H_2SO_4 species. In 2003 Srinivasan et al. [15] included the influence of the electrochemical double layer charge and discharge on the simulation of the pulse charge of VRLA cells subjected to electric (EV) and hybrid vehicle (HEV) operating conditions. They showed that when the effect of the double layer is taken into account, the results obtained in their simulation of short time pulses (in order of magnitude of few seconds or less) are substantially closer to the experimental values.

The technique of the short timed charge or discharge pulses is also used in some methods for state of charge (SOC) and state of health (SOH) evaluation [16–19].

Another application of the pulse charge is its use in the formation of lead-acid battery positive and negative plates [20,21]. The results show that the pulse current accelerates the formation process (electrochemical conversion of PbO , 3BS/4BS and $PbSO_4$ into Pb and PbO_2) and increases its faradic efficiency, i.e. decreases the rate of the water decomposition.

The aim of the present work is to study experimentally the influence of different factors as state of charge, state of health, frequency of the square wave, influence of the double layer, charge and discharge, etc. on the mechanism of the pulse charge of the lead-acid battery positive plates under conditions typical for the PV applications, i.e. mainly low rate charge and discharge currents. The research concentrates on a better understanding of the combined constant current/pulse current charge algorithm proposed recently in Ref. [3].

2. Experimental

The experiments were carried out in three-electrode electrochemical cells consisting of

- working electrode: dry-charged flat positive plate with 3 mm thickness, 8 Ah nominal capacity at 50% positive active mass (PAM) utilization, produced by CEAC-EXIDE (France), with grid composition $Pb-2.8\%Sb$. The plates were cut from bigger 40 Ah plates;
- counter electrode: two dry-charged CEAC-EXIDE (France) negative plates, with nominal capacity 8 Ah and thickness 3 mm. The plates were also cut from bigger 40 Ah plates;

- reference electrode: Ag/Ag_2SO_4 (1.28 s.g. H_2SO_4), +38 mV versus Hg/Hg_2SO_4 in the same solution [22,23].

The electrolyte was H_2SO_4 solution, with a density 1.24 g ml^{-1} . The cells were tested on a SOLARTRON Multistat instrument supplied with Frequency Response Analyzer.

After 30 min of soaking in the electrolyte the cells were subjected to a 20 h charge at $I = 0.25 \text{ A}$ in order to oxidize the residual quantities of $PbSO_4$ unconverted into PbO_2 or Pb during the formation. After this conditioning of the cells, the following cycling regime was applied:

- discharge: $I = -0.8 \text{ A}$ down to $\varphi_{\text{cutoff}}^+ = 0.75 \text{ V}$;
- open circuit: 30 min;
- constant current charge: $I = 0.8 \text{ A}$ up to $\varphi_i^+ = 1.40 \text{ V}$ (interruption potential).
- pulse current charge with $I = 0.8 \text{ A}$ until a 15% of the nominal capacity is introduced. The applied frequency $\omega = T^{-1} = (t_{\text{on}} + t_{\text{off}})^{-1}$ and duty cycle $r = \omega t_{\text{on}}$, were respectively $\omega = 1 \text{ Hz}$ and $r = 0.5$. Here t_{on} and t_{off} are the duration of the charge and the open circuit stay during one square-wave period T .
- 30 min open circuit stay.

3. Results and discussion

3.1. Evolution of the positive plate potential during the pulse charge cycling

Fig. 1 shows the evolution of the current and of the positive plate potential (PPP) versus time during one charge. The comparison of these data with the results reported in [1] shows that the observed cell voltage rise of about 300 mV (from 2.5 to 2.8 V) is due to the increased polarization of the negative plates, because the polarization of the positive plate increases only from 1.4 V to about 1.425 V in the end of the charge. Same results were obtained also during the simultaneous measurements of the evolution of the cell voltage, positive and negative plate potentials. This result demonstrates that the proposed algorithm can be used

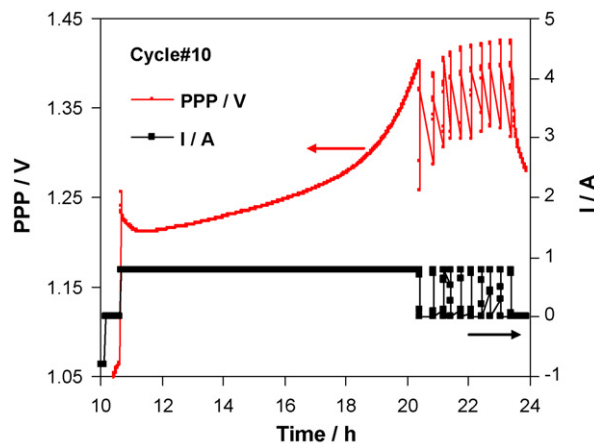


Fig. 1. Positive plate potential and current through the cell during a charge with constant current/pulse current algorithm.

also for charge of VRLA cells, where this limited rise of the positive plate polarization in the end of the charge can cause great benefits in comparison to constant current charge, i.e. decreased oxygen evolution rate and thermal runaway prevention, as well as delay of the positive plate degradation phenomena like grid corrosion and PAM softening.

3.2. Positive plate potential profile during the pulse charge period

Fig. 2 shows the positive plate potential evolution in the beginning and in the end of the pulse charge step (after 10,500 square wave periods, $\omega = 1$ Hz). The increase of the PPP during the ‘ON’ period and the decrease of the PPP during the ‘OFF’ period are about 3 mV. This would suppose that the electrochemical double layer (EDL) participates only slightly in the processes during the pulse charge.

The current of charge and discharge of a capacitor, in our case the EDL, is equal to the product of the capacitance of the EDL and the derivative of the positive plate potential on time

$$I_{DL} = C_{DL} \left(\frac{d\varphi^+}{dt} \right) \quad (1)$$

The average value of the double layer current, $\langle I_{DL} \rangle$, can be defined with the following equation in the case when $t_{on} = t_{off} = 1/2\omega$

$$\langle I_{DL} \rangle = 2\omega \int_0^{1/2\omega} I_{DL} dt \quad (2)$$

$\langle I_{DL} \rangle$ can be used as a simple criterion to evaluate to which extent the EDL participates in the mechanism of the positive plate charge and overcharge in pulse regimes: the higher the value of $\langle I_{DL} \rangle$, the greater the impact of EDL on the charge process. The combination of Eqs. (1) and (2) leads to a very simple expression

$$\langle I_{DL} \rangle = 2\omega C_{DL} (\varphi_{end}^+ - \varphi_0^+) \quad (3)$$

where φ_{end}^+ is the PPP value in the end of the ‘ON’ or ‘OFF’ half-period and φ_0^+ is the PPP value in the beginning of the same ‘ON’ or ‘OFF’ half-period (but after the ohmic jump/drop, respectively).

The change in PPP during the ‘ON’ and ‘OFF’ half-periods ($\Delta\varphi^{ON}$, $\Delta\varphi^{OFF}$) is about 3 mV (Fig. 2). The EDL capacitance

of the used positive plate in completely charged state between cycle#20 and cycle#30 was 100F ($\pm 10F$ variation) measured at open circuit. A detailed explanation and discussion of the EDL capacitance measurement method and the equivalent circuit interpretation of the positive plate structure are given in part 2 of this work, which will consider the impedance of the positive plate in partial SOC [24]. Thus the value of the EDL current will be about 0.6 A, i.e. this current is comparable with the pulse charge current, which is 0.8 A. The high EDL capacitance of the PAM is due to its high surface area. This high current of double layer charge and self-discharge does not support the initial hypothesis that the participation of the EDL in charge mechanism is negligible, regardless of the slight change in PPP. This supercapacitor-type of behavior shows that the future studies of the EDL on the surface of the PbO_2 will be of great importance for the better understanding and the optimization of the pulse charge strategies.

3.3. Influence of the state of charge and OC stay on PPP pulse transients

The influence of the state of charge on the shape of the PPP pulse transients was estimated using the following cycling protocol: the cell was 100% discharged with 0.8 A current. After this, it was subjected to a 120 min OC stay, 7200 s pulse charge as described above and again to 120 min OC stay. This loop of OC and pulse charge was repeated nine times (up to 6.8 Ah totally introduced in the cell).

In Fig. 3 the results are presented for four different SOC values. In the beginning of the charge the changes in the PPP transient are the fastest and the largest, but the EDL capacitance is the lowest. At SOC between 40 and 80% the evolution of the PPP with time is the slightest, and increase little in the end of the charge.

Fig. 4 presents the dependence of the average double layer current $\langle I_{DL} \rangle$ on the SOC of the positive plate. Up to SOC = 70% the $\langle I_{DL} \rangle$ is practically constant, equal to about 25% of the charge current. At higher SOC the $\langle I_{DL} \rangle$ passes through a sharp maximum in the end of the charge. Thus the greatest benefits of the EDL participation in the pulse charge are concentrated in the last 25% of the charge, where $\langle I_{DL} \rangle$ is substantially higher. So in the end of the charge, the primary process is the self-discharge and the charge of the EDL, and the $PbSO_4$ oxidation and the oxygen evolution are consequences of that primary process.

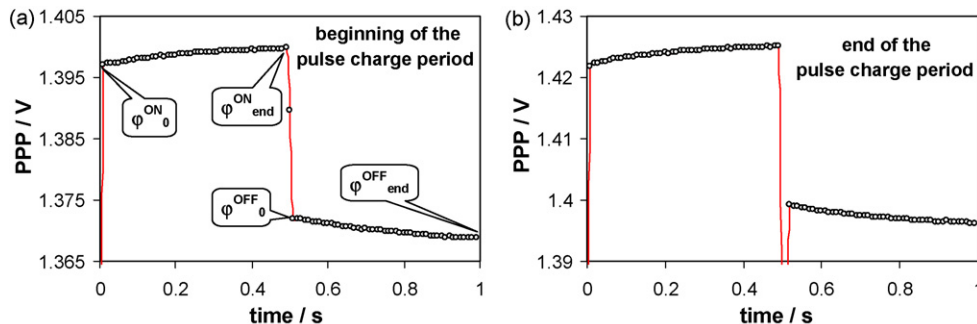


Fig. 2. PPP transients in the beginning (a) and in the end of the pulse charge period (b).

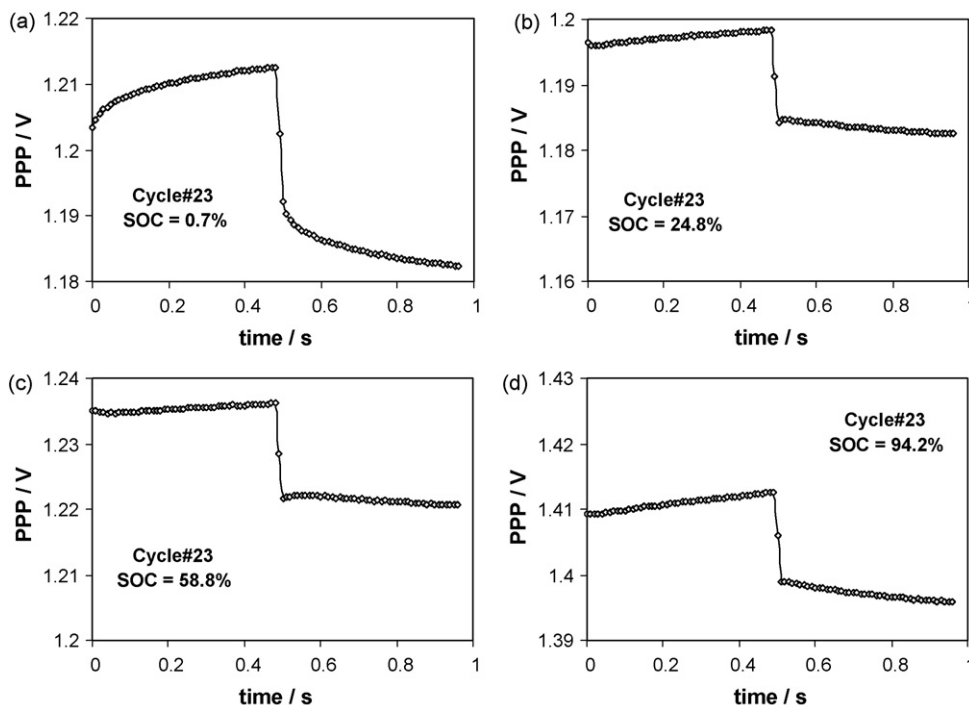


Fig. 3. PPP pulse charge transients at different SOC of the positive plate: (a) 0.7%, (b) 24.8%, (c) 58.8% and (d) 94.2%.

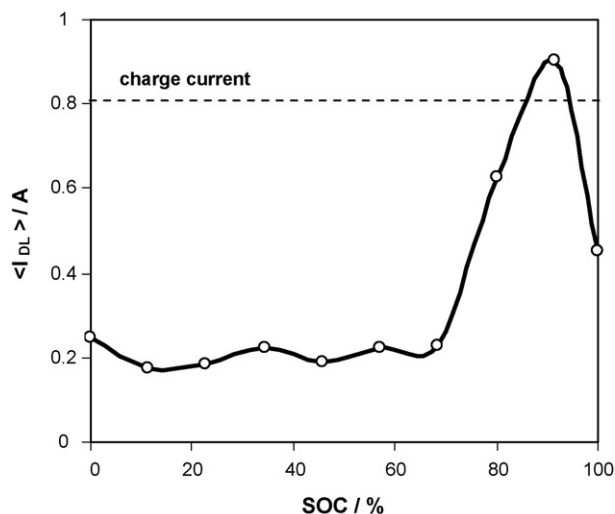


Fig. 4. Dependence of the average double layer current on the SOC of the positive plate.

The comparison of the above described results with PPP transients obtained during pulse charge without the open circuit stays between the pulse series (“continuous” pulse charge) showed that the open circuit stay before each pulse series does not change substantially the character of the PPP pulse transient at the same SOC.

3.4. Electrochemical processes on the positive plate during overcharge with pulse currents

The following experimental protocol was employed to study the O_2 evolution at constant current and at pulse current condi-

tions at 100% SOC: a constant current was applied for period between 1 h (for lower currents) and 5 min (for the highest currents) in order to be reached a steady-state value of the PPP after which a 300 s pulse charge current was applied with $\omega = 1$ Hz and $r = 0.5$. The values of the constant current were between 1 mA and 3.9 A. The pulse current amplitude was equal to the value of the previously applied constant current. The PPP pulse transients for four different values of the overcharge pulse current are shown in Fig. 5.

The correlation between the applied pulse current and the double layer current is obvious—the higher the pulse polarization, the higher the value of the double layer current. This result shows why the pulse charge is so efficient at very high rates: at higher charge rate the double layer participates more actively in the processes of the positive plate charge.

The values of the PPP in the end of the ‘ON’ periods were used to build the $\log(I)$ versus PPP plots (or Tafel plots). The results are shown in Fig. 6. The current taken into account during the pulse periods is the pulse amplitude. It was found that the oxygen overvoltage values do not change from constant current to pulse current mode up to about 80 mA ($0.01C_{10}$), considering the values of the pulse current amplitude. According to Pavlov and Monahov this corresponds to the so-called passive potential zone of the oxygen evolution process [25]. Above 80 mA, the oxygen overvoltage decreases slightly when a pulse current mode of overcharge is applied—the Tafel slope decreases from 145 mV for constant current mode to 136 mV for pulse current mode. This means that the pulse mode facilitates slightly the charge transfer process, hence the mechanism of the electrochemical reactions during the oxygen evolution process will remain the same. On the other side, if we consider the average pulse charge current instead of the pulse

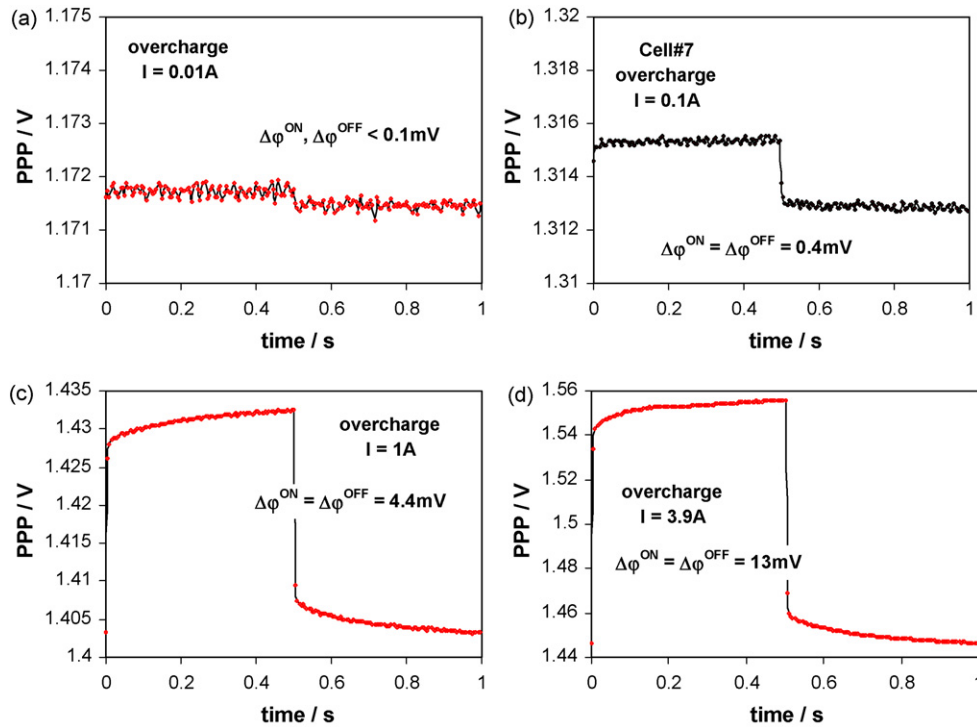


Fig. 5. PPP pulse charge transients at different overcharge pulse currents: (a) 10 mA, (b) 100 mA, (c) 1 A and (d) 3.9 A. The values of the current correspond to the amplitude of the pulse charge.

amplitude the Tafel line will be shifted towards higher values of the potential (the interrupted line in Fig. 6), due to a higher Tafel coefficient “*a*”—from 1032 to 1073 mV (for constant current polarization the *a* = 1023 mV). It can be seen that in this case the pulse mode increases the oxygen overvoltage. The “*a*” coefficient in the Tafel accounts for the number of the active centres. Thus during the pulse charge the number of the active centres participating in the reaction of oxygen evolution is decreased.

Another interesting parameter is the difference of the PPP between the ‘ON’ and the ‘OFF’ periods and its dependence on the overcharge current. This dependence is plotted in Fig. 7. The experimental data obey exactly the Ohm’s law. Hence PPP

drop (or jump) corresponds to the ohmic drop due to the current flowing through the cell as was proposed in [12].

3.5. Impact of the pulse charge frequency on the processes on the positive plate

In Fig. 8 the PPP transients after 500 s pulse charge at frequencies between 10 mHz and 10 Hz are plotted. The pulse charge begins after constant current 0.1 *C*₁₀ charge up to 1.380 V. The time is converted to a dimensionless parameter by multiplication with the corresponding pulse charge frequency. In the beginning of the pulse period (Fig. 8a) the increase in the frequency increases the positive plate polarization. According to the Tafel plot shown in Fig. 6 the oxygen evolution rate in

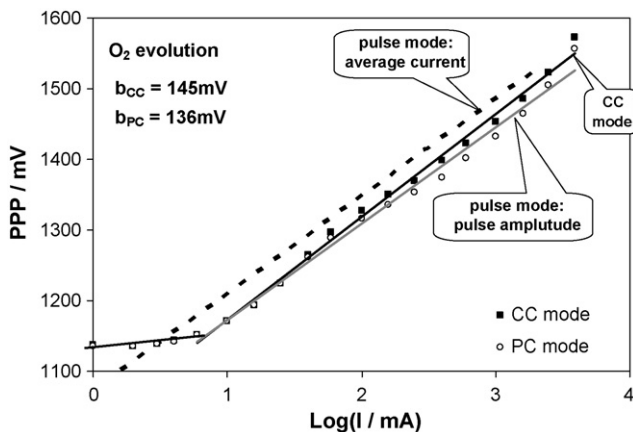


Fig. 6. Tafel plots of the oxygen evolution in constant current (CC) and pulse current (PC) modes of overcharge of the positive plate.

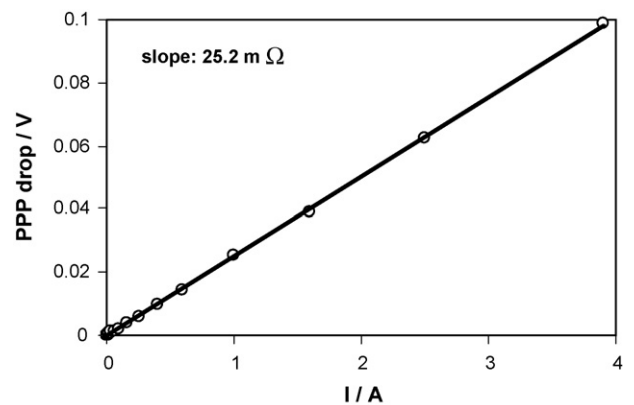


Fig. 7. Dependence of the positive plate potential (PPP) drop in the end of the ‘ON’ half-period of the square wave of the pulse current.

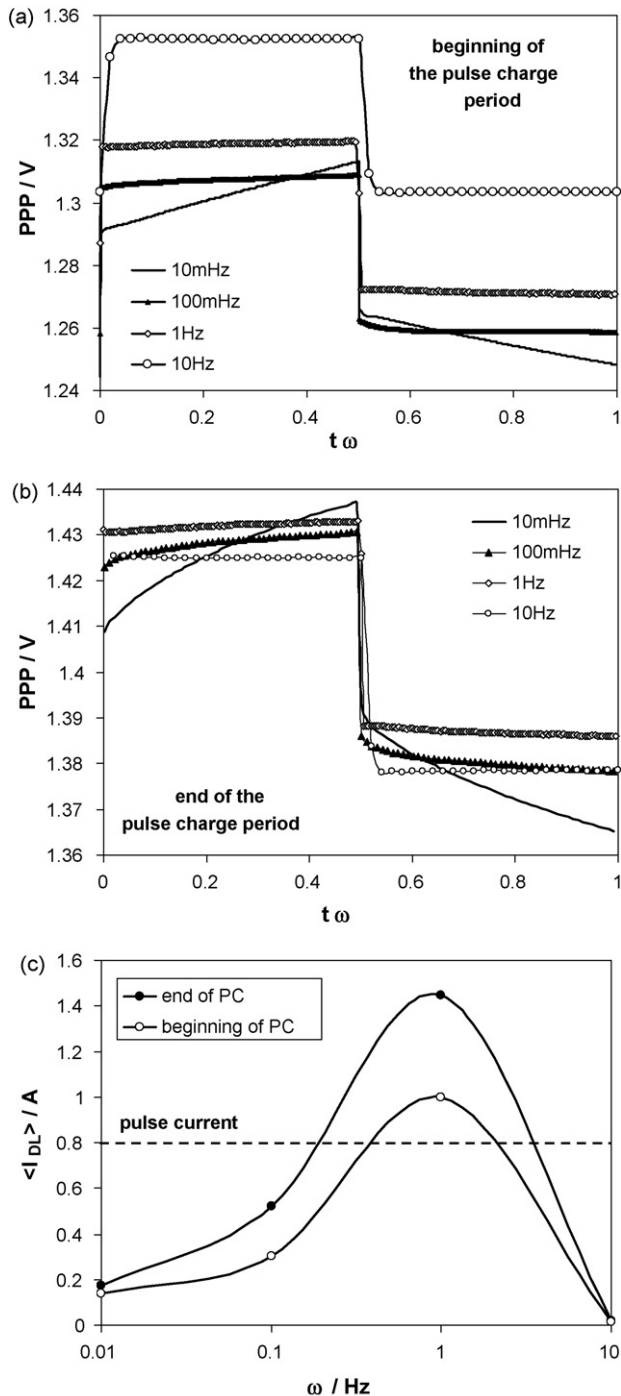


Fig. 8. PPP transients for pulse charge with different frequencies in the beginning (a) and in the end (b) of the pulse period. The x-axis is the dimensionless time—a product of time t and frequency ω . (c) Average double layer current as a function of the pulse current frequency.

this moment will be between 60 and 120 mA, i.e. the charge acceptance is still high and more than 80% of the current corresponds to the process of PbSO_4 oxidation. In the end of the pulse charge period (Fig. 8b) the positive plate is almost completely charged—the partial current of oxygen evolution tends to the overall current flowing through the cell. In this moment the PPP transients for different frequencies are much closer from each other. This result shows that the frequency has a different

influence on the reactions of the positive plate charge and oxygen evolution. Frequencies over 1 Hz increase the polarization of the charge process, i.e. the reaction is hindered (Fig. 8a). An increase of the frequency decreases the oxygen overvoltage (Fig. 8b), i.e. the higher frequency facilitates the oxygen evolution reaction.

The pulse charge frequency impacts also the double layer charge and self-discharge during the “ON” and “OFF” periods. Considering the double layer capacitance, the average double layer current during the “ON” period was calculated. The results are shown in Fig. 8c. It is obvious that the participation of the double layer in the processes of the positive plate charge is maximal at about 1 Hz—this is the point of the highest $\langle I_{DL} \rangle$.

This is the reason why this frequency is optimal for pulse charge with $0.1C_{10}$ pulse current amplitude.

At pulse charge with frequency 1 Hz, the average double layer current exceeds markedly the value of the applied pulse current. Similar result is shown in Fig. 4. The reason for this discrepancy is due to the fact that the double layer capacitance is measured by impedance spectroscopy after 2 h open circuit stay at constant potential equal to the OCP at the end of the this stay, i.e. in steady-state. The capacitance of the double layer during the pulse polarization can differ substantially from the value measured at steady-state—the reasons can be different: non-steady-state adsorption of ions, oxygen evolution/presence of gas bubbles, and chemical reactions on the surface of PbO_2 . It is also important to note that in general the double layer capacitance is function of the electrode potential. The measured C_{DL} values for the four studied frequencies (in the end of each cycle) were between 305 and 331F at SOC = 100%, which means that the variation in C_{DL} values is rather small. Thus even with the exact values of $\langle I_{DL} \rangle$, the shape of the curves from Figure 8c should be very similar and the position of the maximum will remain at 1 Hz. A possible explanation about the origin of the maximum of $\langle I_{DL} \rangle$ at 1 Hz can be found after the comparison of the position of the maximum with the characteristic frequency of the charge transfer process, which is equal to $(2R_{ct}C_{DL})^{-1}$. The typical values of R_{ct} for the studied positive plates are about 2 m Ω [24] and hence the characteristic frequency is about 0.8 Hz. This means that there are conditions for resonance, and maximum of $\langle I_{DL} \rangle$ at 1 Hz can be considered as resonance maximum.

3.6. Impact of the state of health on the pulse charge transients

The PPP transients measured during the cycling of an entire positive plate are shown in Fig. 9a and b in the beginning and in the end of the pulse charge step. The results show that the SOH does not influence substantially the rate of the PPP evolution during the “ON” and “OFF” periods, and hence the average double layer current should not vary in a great extent. However, an interesting result is the substantial evolution in the ratio between charge reaction and oxygen evolution current: in the beginning of the pulse charge step the polarization is highest when the plate is new (i.e. the capacity is highest), but in the end of the step the polarization is highest for the lowest SOH (at cycle#63). Hence in the beginning of the cycling the oxygen evolution process is facilitated and in the end of the life of the

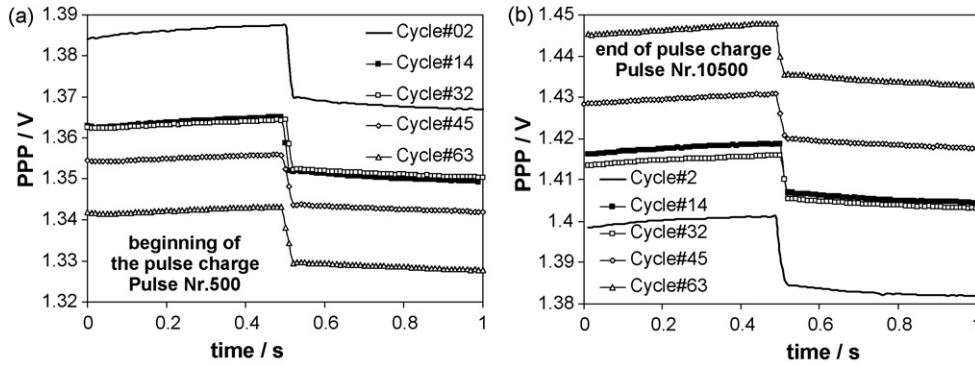
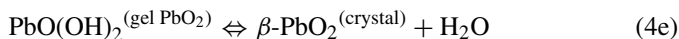
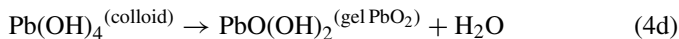
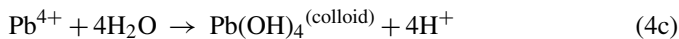
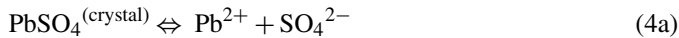


Fig. 9. PPP transients at different cycle numbers: (a) at the beginning of the pulse charge step and (b) at the end of the pulse charge step.

plate the same process is hindered. For the PbSO₄ oxidation rate the situation is opposite.

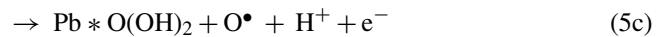
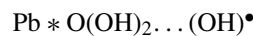
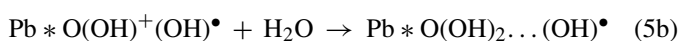
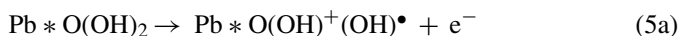
3.7. Mechanism of the process during polarization with pulse charge current

During the positive plate charge with constant current the influence of the double layer is strongly limited in the very beginning of the charge, because the next evolution of the potential is rather slow. Considering the gel–crystal model of the lead dioxide from the positive active material, the mechanism of the PbSO₄ oxidation can be represented by the following reactions [26–29]



The Pb²⁺ ions, dissolved from the PbSO₄ crystals, are oxidized on the surface or in the volume of the gel part of the PbO₂. The latter consists of hydrated polymer chains of lead dioxide, denoted as PbO(OH)₂^(gel PbO₂). The electrochemical reaction (4b) proceeds on determined active centers—these are the places in the hydrated lead dioxide where both electronic and ionic conductivities are maximal. Since the Pb⁴⁺ ions are unstable in water solutions, they react fast with water giving a colloid solution of Pb(OH)₄ (Reaction (4c)). The latter dehydrates partially to hydrated lead dioxide (Reaction (4d)). The hydrated lead-dioxide is in dynamic equilibrium with the one in crystalline state (Reaction (4e)).

During the period of the pulse charge on the positive plate the reaction of oxygen evolution also takes place. This process proceeds on the same active centers located in the gel part of the lead dioxide as Reaction (4c), according to the following mechanism [25]



According to this mechanism the process of oxygen evolution proceeds with the formation of (OH)[•] radicals adsorbed on the active centers by the reactions (5a) and (5b) (“...” denotes the adsorption bond between active center and the OH radical) until the positive plate potential reaches certain value φ_s (~1.3 V vs. Hg/Hg₂SO₄, for PbO₂ formed on flat Pb plate in 0.5 M H₂SO₄ at 25 °C [25]). At φ⁺ < φ_s the active centers are passivated by (OH)[•] radicals and the current of oxygen evolution is quite low. When the positive plate potential exceeds φ_s, the reaction (5c) begins. The produced atoms of oxygen recombine to O₂ (reaction (5d)). The presence of the (OH)[•] radicals as an intermediate in this reaction mechanism was recently confirmed by hydroxyl radical trapping reactions techniques [30].

What happens when the charge current is interrupted? Since the positive plate potential begins to decrease, a self-discharge of the EDL is expected. The values of the average current of EDL self-discharge is comparable with the pulse charge currents because the square waves of the positive plate potential shown in Figs. 2, 3, 5, 8 and 9 are almost symmetric

$$\frac{d\varphi_{\text{ON}}^+}{dt} \approx -\frac{d\varphi_{\text{OFF}}^+}{dt} \quad (6)$$

i.e. the rates of EDL charge is almost equal to the rate of EDL self-discharge. At the same time, during the “OFF” period, the positive plate potential remains much higher than the steady-state potential of the positive plate at open circuit and of course much higher than the equilibrium potential of the PbO₂/PbSO₄ electrode (1.05 V vs. Ag/Ag₂SO₄ in H₂SO₄ with density 1.24 g/ml [22]). The potential is also high enough to maintain the process of oxygen evolution with a substantial rate (see the Tafel plots shown in Fig. 6). So the energy dissipated during the self-discharge of the double layer in the “OFF” period should be utilized by some of the above-mentioned Faradic processes—the electrochemical reactions (4b), (5a) and (5c). This mechanism of coupled supercapacitor self-discharge with Faradic reactions is discussed in details in the works of Conway et al. [31,32] and is used further in the simulation of pulse charge

of VRLAB [15]. According to Conway [31,32], if the EDL self-discharge is coupled with a Faradic process, the electrode potential at open circuit should obey the equation

$$I_{DL} = -C_{DL} \left(\frac{d\varphi^+}{dt} \right) = I_0 \exp \left(\frac{n\alpha F\varphi^+}{RT} \right) \quad (7)$$

where the term $(RT/2.303n\alpha F)$ is equivalent to the Tafel slope $b_{CC/PC}$ from Fig. 6, α is the charge transfer coefficient, n is the number of charges participating in the reaction, T is the temperature, R and F are the molar and the Faradic constants. The open circuit decay transients of the positive plate potential are plotted in Fig. 10a for different values of SOC. The experimental conditions were mentioned in Section 3.3 “Influence of the state of charge and OC stay on PPP pulse transients”. These data were used to calculate the dependences of the $\log(d\varphi^+/dt)$ versus φ^+ shown in Fig. 10b. The analysis of the results shows that at SOC <75% this dependence is linear and the Tafel slope is between 19 and 20 mV (denoted as b_1 in Fig. 10b). At higher SOC the dependence of $\log(d\varphi^+/dt)$ on φ^+ consists of three parts with different Tafel slopes—20 mV for lower values of

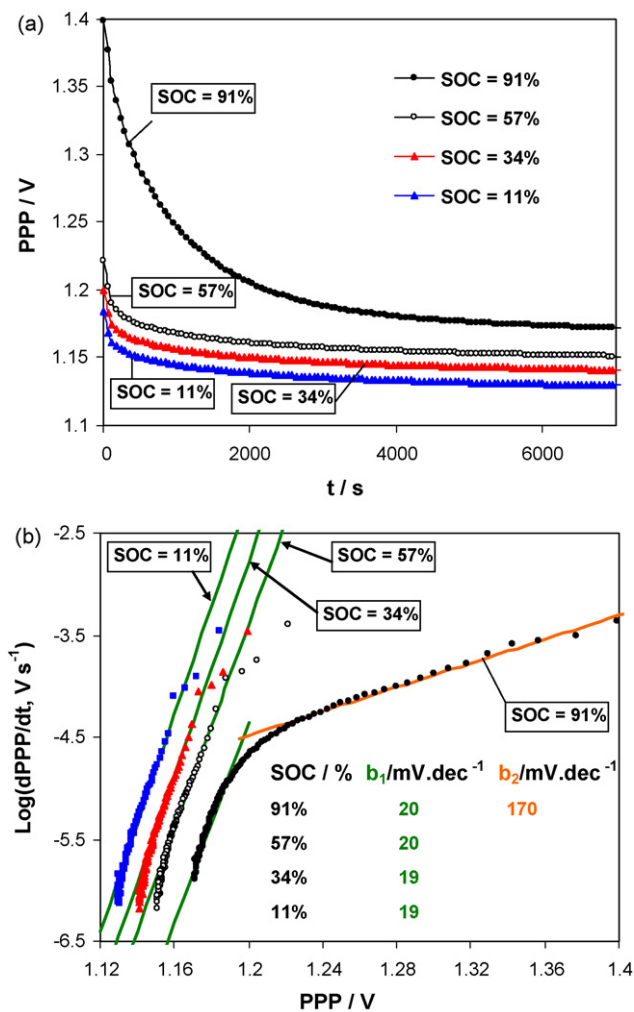


Fig. 10. (a) Positive plate potential open circuit decay transients at different SOC. (b) $\log(dPPP/dt)$ vs. positive plate potential dependence, the straight lines correspond to a linear fit.

φ^+ , 170 mV for $\varphi^+ > 1.22$ V, and transition region between 1.18 and 1.22 V where the slope is 66 mV. These results show what is the mechanism of self-discharge of the EDL:

- At SOC <75% the EDL self-discharge process is coupled with a Faradic process with facilitated charge transfer, due to the low value of the Tafel slope of 19–20 mV. Such process is the oxidation of the $PbSO_4$ to PbO_2 , i.e. the electrochemical reaction (4b).
- At higher SOC, the low polarization part keeps approximately the same Tafel slope of 20 mV, which is an indication that the preferred reaction is still an oxidation of the $PbSO_4$ to PbO_2 . The value of 170 mV for the Tafel slope in the earliest stages of the open circuit potential decay at high SOC is close to the values of the Tafel slope obtained during the positive plate polarization with constant and pulse currents, shown in Fig. 4, which are 145 mV for the constant current mode and 136 mV for the pulse current mode. Hence it is obvious that in the earlier moments of the open circuit stay the self-discharge of the EDL is coupled with the process of oxygen evolution.
- In the transition region between 1.18 and 1.22 V, where the Tafel slope is 66 mV, we have a mixed potential corresponding to the simultaneous proceeding of the reactions (5a–b) and (4b). The same transition region of mixed potential corresponds to the first 2–3 points (the first 2 min after the current interruption) at lower SOC.

Regardless of the obtained results for the oxygen evolution in the regime of pulse charge (e.g. this process continues during the “OFF” periods and even is slightly facilitated) the pulse charge regime increases the faradic efficiency of the charge [3,7,8,10–13] and even of the positive plate formation [20,21]. The increased Faradic efficiency can result only in a decreased oxygen evolution rate, while the mechanism stays unchanged. The only possible way to decrease the rate of the oxygen evolution is the trapping of the intermediates of the oxygen evolution (O atoms and OH radicals) by species which can be oxidized. Such species are only the Pb(II) ions in the solution near the interface PbO_2 /electrolyte. During the “OFF” period, the rate of the electrochemical reactions is equal to the rate of the EDL self discharge, which in general is less than the amplitude of the pulse current. Additionally the decreased polarization due to the pulse current decreases the oxygen evolution rate. During the “ON” period, most of the current is consumed for the recharge of the EDL, instead of the proceeding of the oxygen evolution. Hence the process of the oxygen evolution is “expanded” in the time, and the flow of O atoms and OH radicals is decreased. Thus the processes of the radicals’ recombination leading to formation of molecular oxygen are delayed. On the other hand the flow of Pb(II) ions from the dissolution of the lead sulphate remains rather constant because the reaction (4a) is a chemical process, which rate does not depend on the applied polarization. So during the pulse charge period a substantial part of the Pb(II) ions in the system will have more time to participate in chemical reactions of the following type





Such type of reactions is very fast because it is well known that the O atoms and the OH radicals are strong oxidizing agents. Reactions (8a) and (8b) stop the formation of molecular oxygen, which is less reactive and easily escapes the positive plate pores in gaseous form, and increase the Faradic efficiency of the charge and formation, because of the lead dioxide deposition.

4. Conclusions

1. The positive plate potential evolution in pulse charge regime is much slower than that of the negative plate, resulting in quasi flat-shaped PPP transients. Nevertheless, due to the high EDL capacitance of the PAM, even a small increase or decrease in the PPP during one half-period of the pulse square wave results in a substantial capacitive charge or self-discharge current. In order to evaluate the extent of participation of the EDL in the process of positive plate pulse charge, the term average double layer current, $\langle I_{DL} \rangle$, was used.
2. The results obtained regarding the dependence of $\langle I_{DL} \rangle$ versus SOC show that the application of a pulse charge is particularly efficient in the end of the charge. There, the $\langle I_{DL} \rangle$ has maximum values.
3. The overcharge with pulse currents showed that the pulse polarization does not change the electrochemical steps in the mechanism of the oxygen evolution, but the increase of the overcharge current amplitude increases substantially the average double layer current, which explains the successful fast charge (30–60 min full charge) with pulse currents.
4. The results obtained about the influence of the pulse frequency on the pulse charge efficiency showed that it will be maximal at 1 Hz due to the maximum of the $\langle I_{DL} \rangle$ at this frequency. The increase or decrease of this frequency leads to sharp decrease of the $\langle I_{DL} \rangle$.
5. The SOC does not exert a substantial influence on the character of the PPP transients during the “ON” and “OFF” periods, but changes the ratio “charge reaction/oxygen evolution” in the beginning and in the end of the pulse charge step.
6. The study of the mechanism of the EDL self-discharge showed that this process is coupled with the lead sulphate oxidation reaction when the positive plate potential is below 1.2 V, and with the oxygen evolution process when the potential is higher than 1.2 V. Hence the higher faradic efficiency during the pulse charge should be related to the chemical oxidation of Pb(II) ions by O atoms and OH radicals which are produced on the PbO₂ surface by the oxygen evolution both during the “ON” and “OFF” periods.

References

- [1] F. Mattera, D. Benchetrite, D. Desmetre, J.L. Martin, E. Potteau, J. Power Sources 116 (2003) 248–256.
- [2] R.F. Nelson, E.D. Sexton, J.B. Olson, M. Keyser, A. Pesaran, J. Power Sources 88 (2000) 44–52.
- [3] D. Benchetrite, M. Le Gall, O. Bach, M. Perrin, F. Mattera, J. Power Sources 144 (2005) 346–351.
- [4] W.B. Burkett, The Rapid Charging of Batteries, BCI, Phoenix, AZ, April, 1972.
- [5] R.H. Sparks, SAE Pap. 720109 for meeting, 1 January, 1972, p. 12.
- [6] J.J. Smithrick, NASA Tech. Memo., September, 1981, p. 9.
- [7] L.T. Lam, H. Ozgun, O.V. Lim, J.A. Hamilton, L.H. Vu, D.G. Vella, D.A.J. Rand, J. Power Sources 53 (1995) 215–228.
- [8] J.A. Wilkinson, G.A. Covic, Transactions of the Institution of Professional Engineers New Zealand, Electrical, Mechanical, and Chemical Engineering Section 25 (1998) 1–11.
- [9] M. Bhatt, W.G. Hurley, W. Wolfle, Proceedings of the Universities Power Engineering Conference, vol. 37, 2002, pp. 477–481.
- [10] L.T. Lam, N.P. Haigh, C.G. Phyland, T.D. Huynh, J. Power Sources 53 (1995) 215–228.
- [11] Q.-H. Wang, L. Li, L.-P. Jin, Q. Zhou, Chin. J. Power Sources 26 (2002) 336–338.
- [12] R. Groß, H. Döring, J. Garche, Z. Phys. Chem. 208 (1999) 253–266.
- [13] Y. Guo, R. Groiss, H. Doering, J. Garche, J. Electrochem. Soc. 146 (1999) 3949–3957.
- [14] S.C. Kim, W.H. Hong, J. Power Sources 89 (2000) 93–101.
- [15] V. Srinivasan, G.Q. Wang, C.Y. Wang, J. Electrochem. Soc. 146 (1999) A316–A325.
- [16] T. Ogata, K. Takano, M. Kohno, K. Yoshida, Electron. Commun. Jpn. Part I: Commun. 77 (1994) 1–10.
- [17] K. Yamamoto, T. Ogata, K. Takano, K. Yoshitaka, NTT Rev. 7 (1995) 65–69.
- [18] B. Le Pioufle, J.F. Fauvarque, P. Delalande, Eur. Phys. J. AP 2 (1998) 257–265.
- [19] D. Pavlov, G. Petkova, J. Electrochem. Soc. 149 (2002) A644.
- [20] L.T. Lam, H. Ozgun, L.M.D. Cranswick, D.A.J. Rand, J. Power Sources 42 (1993) 55–70.
- [21] F.B. Diniz, L.E.P. Borges, B.de B. Neto, J. Power Sources 109 (2002) 184–188.
- [22] P. Ruetschi, J. Power Sources 116 (2002) 53.
- [23] P. Ruetschi, J. Power Sources 113 (2002) 363.
- [24] A. Kirchev, A. Delaille, M. Perrin, E. Lemaire, F. Mattera, J. Power Sources 170 (2007) 495.
- [25] D. Pavlov, B. Monahov, J. Electrochem. Soc. 143 (1996) 3616.
- [26] D. Pavlov, in: D.A.J. Rand, P.T. Moseley, J. Garche, C.D. Parker (Eds.), Formation of Lead-Acid Batteries and Structure of the Positive and Negative Active Masses, Elsevier, Amsterdam, 2004, p. 70, chapter 3.
- [27] D. Pavlov, J. Electrochem. Soc. 139 (1992) 3075–3080.
- [28] D. Pavlov, I. Balkanov, J. Electrochem. Soc. 139 (1992) 1830–1835.
- [29] D. Pavlov, I. Balkanov, T. Halachev, P. Rachev, J. Electrochem. Soc. 139 (1992) 3189–3197.
- [30] S. Ai, Q. Wang, H. Li, L. Jin, J. Electroanal. Chem. 578 (2005) 223–229.
- [31] B.E. Conway, J. Electrochem. Soc. 138 (1991) 1539–1548.
- [32] J. Niu, B.E. Conway, W.G. Pell, J. Power Sources 135 (2004) 332–343.